J. Condensed Matter Nucl. Sci. 15 (2015) 149–161

Research Article

Piezonuclear Fission Reactions Simulated by the Lattice Model

A. Carpinteri*, A. Manuello and D. Veneziano

Politecnico di Torino, Department of Structural, Geotechnical and Building Engineering, Corso Duca degli Abruzzi, 24–10129 Torino, Italy

N.D. Cook†

Kansai University, Department of Informatics, Takatsuki, Osaka 569-1095, Japan

Abstract

Recent experiments conducted on natural rocks subjected to different mechanical loading conditions have shown energy emissions in the form of neutrons and anomalous chemical changes. In the present study, a numerical model is used to simulate the anomalous nuclear products according to the fission interpretation. Specifically, the reactions were simulated by means of a nuclear lattice model assuming that nucleons are ordered in an antiferromagnetic face-centered-cubic (fcc) array. The simulations indicate that small and middle-sized nuclei can be fractured along weakly bound planes of the lattice structure. It is argued that the simulations provide theoretical support for the experimentally-observed reactions and, moreover, that the probabilities calculated for various low-energy fissions can be used to explain the stepwise changes in the element abundances of the Earth's crust, evolved from basaltic to sialic composition over geological time.
 ISSN 2227-3123

Keywords: Earth crust composition, Lattice model, Nuclear cold fusion, Piezonuclear fission reactions

1. Introduction

In the last few years, numerous experiments have been conducted on natural non-radioactive rocks, such as granite, basalt, magnetite and marble, by subjecting them to different mechanical loading conditions. The experiments were always accompanied by energy emissions and anomalous chemical changes [1–8] and provided repeatable evidence concerning a new kind of nuclear reaction that may take place during quasi-static or cyclic-fatigue tests at low (2 Hz), intermediate (200 Hz) and high (20 kHz) loading frequencies [8]. Such evidence indicates that mechanical pressure waves, suitably exerted on an inert medium of stable nuclides, can generate neutron emissions and nuclear reactions of a new type [1–14].

Very recently, theoretical interpretations have been proposed by Widom et al. in order to explain neutron emissions as a consequence of nuclear reactions taking place in iron-rich rocks during brittle micro-cracking and fracture [13,14].

*E-mail: alberto.carpinteri@polito.it
†E-mail: cook@res.kutc.kansai-u.ac.jp

 ISSN 2227-3123

Several evidences show that iron nuclear disintegrations are observed when rocks containing such nuclei are crushed and fractured. The resulting nuclear transmutations are particularly evident in the case of magnetite rocks and iron-rich materials in general. The same authors argued that neutron emissions may be related to piezoelectric effects and that fission of iron may be a consequence of the photodisintegration of the same nuclei [13].

Those experimental results together with the evidence of so-called low-energy nuclear reactions (LENR) [15–17] strongly suggest that knowledge of nuclear structure is not a "closed chapter" in Physics. Moreover, recent studies on piezonuclear fission reactions, occurring in the Earth's crust and triggered by earthquakes and brittle rocks failure, provide a good opportunity for old questions concerning nuclear structure to be addressed once again in the light of new phenomena suggestive of low-energy nuclear reactions [12]. Even small deviations from conventional assumptions, e.g., concerning the condensation density of nuclear matter or the concept of an average binding energy per nucleon [15,18–22], could have significant implications. Based on the experimental evidence concerning piezonuclear fission, it would suffice to assume that a nuclear structure failure occurs along weak lattice planes within the nucleus, similar to the cleavage fractures known to occur in very hard and strong rocks [6–8].

The nuclear lattice model has been advocated by Cook and Dallacasa as a unification of the diverse models used in nuclear structure theory [17–19,23–30], but, remarkably, the basic lattice structure was first proposed by the originator of the well-established independent-particle model, Eugene Wigner, in 1937 [31] – work that was explicitly cited in his Nobel Prize notification. The lattice model has previously been used to simulate (i) the mass of fission fragments produced by thermal fission of the actinides, and (ii) the transmutation products found on palladium cathodes after electrolysis, as reported in various experimental studies [20,29,30,32]. With regard to the underlying nuclear lattice model, the antiferromagnetic face-centered-cubic (fcc) lattice with alternating proton and neutron layers is the most suitable model for various reasons: (i) from theoretical research on nuclear matter, it is known to be the lowest-energy solid-phase packing scheme of nucleons ($N = Z$) [17–19,22]; (ii) the lattice structure reproduces the quantum number symmetries of the independent particle model (IPM) (the entire n-shell and j-lm-subshells of the shell model), while being based on the local interactions of the liquid drop model (LDM) [17,21,22]; (iii) because of the identity between the nuclear lattice and the IPM, the approximate nucleon build-up procedure is known and implies a specific 3D structure for any given number of protons and neutrons with known quantum numbers, which can be represented in Cartesian space [17].

Several decades of development of the lattice model suggest that the gaseous, liquid, and cluster-phase models of conventional nuclear structure theory can be unified within a specific lattice model. Moreover, the lattice lends itself to straightforward application in explaining different fission modes [17,21,22]. The earlier simulation results were concerned with fission fragments from uranium nuclei and transmutation products from palladium isotopes (experimentally reported by Mizuno in 1998 and 2000 [20,32]). In the present simulations, the Nuclear Visualization Software (NVS) [17] was used to simulate the anomalous nuclear reactions recently observed by Carpinteri et al. [1–11] and to numerically reproduce the nuclear products observed after fracture and fatigue experiments. The results lead to the conclusion that the anomalous nuclear reactions, emerging from Energy Dispersive X-ray Spectroscopy (EDS) analysis of fractured specimens and from the evolution of the continental Earth's crust, can be well explained by the nuclear lattice model. In addition, the lattice approach allows one to compute a probability related to each possible fission reaction. The probability values obtained for the anomalous reactions can then be used to interpret the evolution of the abundance of product elements in the Earth's crust, ocean and atmosphere.

2. Reproducing Anomalous Fission Fragments using the Lattice Model

The nuclear lattice model proposed by Cook and Dallacasa [17–19,23–28] can be used to simulate the piezonuclear fission reactions by constructing individual isotopes, in accordance with the lattice build-up procedure, and then simulating the cleavage of the lattice along various lattice planes. The starting points for the simulations are therefore

the nuclear structures of the elements and those known to be abundant in the Earth's crust today and in previous eras [6–12]. Although other nuclear structure models have been developed since the 1930s, the fcc lattice is the most suitable to simulate the anomalous reactions recently discovered because of its clear structural implications. The simulation begins with a 3D lattice structure of specific isotopes based on the total number of neutrons N and protons Z. By simulating the fission of the nucleus as a fracture occurring along a certain section plane across the lattice, "fragments" are produced, and correspond to the post-fission daughter nuclei.

The quantum mechanical foundations of the lattice model and its relation to the Schrödinger wave-equation have been discussed elsewhere, but, for the purposes of the simulation, it is sufficient to describe the lattice structure in Cartesian space. That is, the mean position of each nucleon can be defined in relation to its quantum numbers by means of the following equations [17]:

$$x = |2m|\,(-1)\,(m + 1/2)\,, \tag{1}$$

$$y = (2j + 1 - |x|)\,(-1)^{(i+j+m+1/2)}\,, \tag{2}$$

$$z = (2n + 3 - |x| - |y|)\,(-1)^{(i+n-j-1)}\,, \tag{3}$$

where n, m, j, s, and i are the quantum numbers that describe the energy state for a given nucleon [21,22]. Equations (1)–(3) are deduced from a rigorous, self-consistent representation of the IPM in three-dimensional space [17]. In accordance with the known quantum mechanics of nuclear states, each nucleon is characterized by a unique set of five quantum numbers, which define the precise energy state of the nucleon, as described by the Schrödinger equation [17,21,22]. The spatial origin of this wave is a function of the three coordinates x, y, z. Hence, for any isotope, knowing that each nucleon belongs to a certain energy level given by the values of its quantum numbers, it is possible to consider the 3D lattice of nucleons as a representation of its quantum mechanical state [17,21,22].

Piezonuclear reactions cannot be defined as traditional fission reactions, since temperature and energy conditions are not equivalent to those involved in thermal neutron-induced fission. For this reason, it is convenient to verify that these anomalous reactions may be correctly described in the NVS simulations. To simulate this new kind of fission, we assumed that fractures occur in the nuclear lattice along their crystal planes. Following this approach, two distinct fragments are produced from any considered reaction. Their characteristics are given by the NVS in terms of fragment stability, fission threshold energy along a certain fracture plane, and the number of protons and neutrons in each fragment. The resulting elements can be deduced from the characteristics of the fragments obtained at the end of the simulation. The analysis of the nuclear characteristics is described in the next section along with the isotopes obtained from the piezonuclear reactions. Important considerations are made on the neutron emissions from the anomalous nuclear reactions measured during the experiments. They may be deduced by investigating the stability of the resulting fragments. We assume that unstable isotopes with an excess of neutrons are likely to induce neutron emissions, depending on local binding characteristics, in order to reach more stable nuclear states. These emissions deduced from the model are then compared with the experimental results reported by Carpinteri et al. [1–11].

3. Simulations and Results

The NVS simulates lattice structures up to 480 nucleons and calculates fission results along 17 different section planes for each given nuclide (Table 1). In fact, many more lattice planes are available for simulation, but the electrostatic repulsion between the protons in the two fragments is much greater for lattice planes that break the lattice structure into

Table 1. Fission planes and their identification number in the NVS.

Fracture plane	Equations
1	$x = 2$
2	$x = 0$
3	$x = -2$
4	$z = -2$
5	$z = 0$
6	$z = 2$
7	$y = 2$
8	$y = 0$
9	$y = -2$
10	$-x + y + z + 1 = 0$
11	$-x + y + z - 1 = 0$
12	$x - y + z + 1 = 0$
13	$x - y + z - 3 = 0$
14	$-x - y + z - 1 = 0$
15	$-x - y + z + 3 = 0$
16	$x + y + z - 1 = 0$
17	$x + y + z + 3 = 0$

approximately symmetrical fragments, so that many low-repulsion, asymmetrical fission events are ignored. A single simulation consists in fracturing the nucleus along one single plane at a time, breaking only the bonds that connect the two fragments [17]. It is understandable that the choice of the fracture planes is affected by the lattice structure and, therefore, by the position of the nucleons with respect to the x, y, z axes. Being a lattice model drawn from crystallography implies that all the planes used for the simulations correspond to the principal crystallographic planes [17]. In particular, the seventeen planes used by the NVS are parallel to the horizontal, vertical and inclined (45°) planes passing through or near the origin of the axes. Each plane is identified by a number from 1 to 17, as shown in Table 1.

Eighteen reactions derived from direct and indirect experimental evidence were simulated by means of the NVS along different fission planes and each considering a different starting element (Table 2). As mentioned in Section 1, the elements known to be involved in the piezonuclear reactions were considered in the numerical simulations. Such reactions are strictly connected to: (i) the experimental results obtained from the EDS analyses performed after fracture tests on natural rock specimens, or (ii) the compositional changes in the Earth's crust evolution during the last 4.57 billion years [5–12]. As recently reported [9–12], the evolution of the Earth's crust and atmosphere, the formation of oceans and greenhouse gases, and the origin of life are phenomena deeply related to piezonuclear reactions [1–12]. This was the motivation for undertaking the simulation of fission reactions according to a non-traditional methodology [19].

These reactions were simulated using two build-up procedures for nuclear structure. The first one generates a default nucleus where each nucleon has a pre-assigned position and quantum numbers that give the lattice a regular, densely-packed, polyhedral structure. The second procedure uses the "picking function", which is the most convenient way for constructing a nucleus from a set of nucleons with specific quantum numbers and coordinates [17]. The picking function was applied only when the lattice structures using the default configuration were inappropriate due to the weak bonding of the last few nucleons. In particular, once a specific default nucleus has been constructed and displayed, usually the last two protons or neutrons were individually moved from one energy-state to another to find the configuration that best reproduces the (fission) product elements.

All 18 reactions reported in Table 2 are simulated by the NVS and the results are summarized in Table 3. For

Table 2. Piezonuclear reactions obtained as direct evidence from EDS analysis of fractured specimens, or conjectured considering the continental Earth's crust evolution.

Earth's crust evolution	
(1)	$Fe_{26}^{56} \rightarrow 2\ Al_{13}^{27} + 2$ neutrons
(2)	$Fe_{26}^{56} \rightarrow Mg_{12}^{24} + Si_{14}^{28} + 4$ neutrons
(3)	$Fe_{26}^{56} \rightarrow Ca_{20}^{40} + C_{6}^{12} + 4$ neutrons
(4)	$Co_{27}^{59} \rightarrow Al_{13}^{27} + Si_{14}^{28} + 4$ neutrons
(5)	$Ni_{28}^{59} \rightarrow 2\ Si_{14}^{28} + 3$ neutrons
(6)	$Ni_{28}^{59} \rightarrow Na_{11}^{23} + Cl_{17}^{35} + 1$ neutron
Atmosphere evolution, ocean formation and origin of life	
(7)	$Mg_{12}^{24} \rightarrow 2C_{6}^{12}$
(8)	$Mg_{12}^{24} \rightarrow Na_{11}^{23} + H_{1}^{1}$
(9)	$Mg_{12}^{24} \rightarrow O_{8}^{16} + 4H_{1}^{1} + 4$ neutrons
(10)	$Ca_{20}^{40} \rightarrow 3C_{6}^{12} + He_{2}^{4}$
(11)	$Ca_{20}^{40} \rightarrow K_{19}^{39} + H_{1}^{1}$
(12)	$Ca_{20}^{40} \rightarrow 2O_{8}^{16} + 4H_{1}^{1} + 4$ neutrons
Greenhouse gas formation	
(13)	$O_{8}^{16} \rightarrow C_{6}^{12} + He_{2}^{4}$
(14)	$Al_{13}^{27} \rightarrow C_{6}^{12} + N_{7}^{14} + 1$ neutron
(15)	$Si_{14}^{28} \rightarrow 2\ N_{7}^{14}$
(16)	$Si_{14}^{28} \rightarrow C_{6}^{12} + O_{8}^{16}$
(17)	$Si_{14}^{28} \rightarrow 2C_{6}^{12} + He_{2}^{4}$
(18)	$Si_{14}^{28} \rightarrow O_{8}^{16} + 2He_{2}^{4} + 2H_{1}^{1} + 2$ neutrons

each simulation, the plane that allows the anomalous fission is indicated. Each fragment is identified by the number of protons (Z), the number of neutrons (N), and the corresponding isotope. In addition, when the fragment is unstable, NVS displays the experimentally known decay time of that fragment. In the case of unstable fission fragments, the number of neutrons exceeds the stable condition and neutron emissions may occur from that fragment in order to achieve stability. It is interesting to note that, from the NVS results, it is possible to reproduce the neutron emissions of piezonuclear reactions, in addition to the product elements (fragments).

For the first simulation, the Fe_{26}^{56} nucleus was chosen as the starting element and the lattice of this nucleus is shown in Fig. 1. Its characteristics assigned by the software are as follows: Protons: 26; Neutrons: 30; n-values: 0, 1, 2, 3; j-values: 1/2, 3/2, 5/2, 7/2; m-values: $\pm$1/2, $\pm$3/2, $\pm$5/2, $\pm$7/2, according to the literature [17,21,22].

Once the nuclear structure is modified with the picking option, the lattice is "fractured" along fission planes that cut all nucleon–nucleon bonds connecting the two fragments (Fig. 2). Among the 17 planes of fission, six of them are relevant for reactions (1)–(3) of Table 2, whereas the remaining 11 produce results unrelated to the empirical data (Table 2). Specifically, the simulation results related to reaction (1) occur along the fission planes 2 and 8, which are the *yz* and the *xz* plane in Cartesian space respectively (see Table 1 and Fig. 2). As shown in Table 4, the fragments produced from the fissions along planes 2 and 8 possess the same characteristics as those described in the piezonuclear reaction (1) (Table 2). The two fragments correspond toAl_{13}^{27}, andAl_{13}^{29}. The former is stable, whereas the latter is unstable as it contains two neutrons in excess, which are weakly-bound to the lattice fragment and are presumably emitted when the reaction occurs. Assuming the emission of these two neutrons, the fission can be considered as symmetric with respect to both planes 2 and 8.

The second simulation was run in accordance with reaction (2) (see Table 2 and Table 3). In this case, the lattice structure forFe_{26}^{56} is produced using the picking option [17]. The fragments obtained from the fission simulated by

Table 3. Fracture of the Mg^{24} lattice along plane 2; broken bonds are represented in red between the fragments of reaction (7) in Table 3.

Reaction	Plane	Fragment 1					Fragment 2					Neutron Emission	Fission Probability (%)
		Z	N	A	Isotope	Decay time[1]	Z	N	A	Isotope	Decay time[1]		
(1)[2]	2	13	14	27	Al^{27}	Stable	13	16	29	Al^{27}	6.6 (m)	+2n	23.22
	8	13	14	27	Al^{27}	Stable	13	16	29	Al^{27}	6.6 (m)	+2n	
(2)[2]	14	12	12	24	Mg^{24}	Stable	14	18	32	Si^{28}	172(y)	+4n	40.74
	16	12	12	24	Mg^{24}	Stable	14	18	32	Si^{28}	172(y)	+4n	
(3)[2]	1	6	7	13	C^{12}	Stable	20	23	43	Ca^{40}	Stable	+4n	36.04
	3	20	22	42	Ca^{40}	Stable	6	8	14	C^{12}	5730(y)	+4n	
(4)	2	13	14	27	Al^{27}	Stable	14	18	32	Si^{28}	172 (y)	+4n	100
	8	14	16	30	Si^{28}	Stable	13	16	29	Al^{27}	6.6 (m)	+4n	
(5)[2]	2	14	16	30	Si^{28}	Stable	14	15	29	Si^{28}	Stable	+3n	32.60
(6)[2]	12	11	13	24	Na^{23}	14.95(h)	17	18	35	Cl^{35}	Stable	+n	67.40
(7)[2]	2	6	6	12	C^{12}	Stable	6	6	12	C^{12}	Stable		11.26
(8)[1]	9	11	12	23	Na^{23}	Stable	1	0	1	H^{1}	Stable		31.01
(9)[2]	4	8	12	20	O^{16}	13.5(s)	4	0	4	$4H^{1}$	Stable	+4n	
	6	0	4	4			12	8	20	O^{16}+$4H^{1}$	0.1(s)	+4n	
	7	4	4	8	$4H^{1}$	0.07(fs)	8	8	16	O^{16}	Stable	+4n	(57.73)
	8	8	9	17	O^{16}	Stable	4	3	7	$4H^{1}$	0.07(fs)	+4n	
(10)[2]	1	2	2	4	He^{4}	Stable	18	18	36	$3C^{12}$	Stable		10.28
(11)[2]	1	1	0	1	H^{1}	Stable	19	20	39	K^{39}	Stable		58.46
	1	4	4	8	$4H^{1}$	0.07(fs)	16	16	32	$2O^{16}$	Stable	+4n	
(12)	3	16	16	32	$2O^{16}$	Stable	4	4	8	$4H^{1}$	0.07(fs)	+4n	31.26
	7	4	4	8	$4H^{1}$	0.07(fs)	16	16	32	$2O^{16}$	Stable	+4n	
	9	16	16	32	$2O^{16}$	Stable	4	4	8	$4H^{1}$	0.07(fs)	+4n	
(13)[2]	13	6	6	12	C^{12}	Stable	2	2	4	He^{4}	Stable		100
(14)	2	6	7	13	C^{12}	Stable	7	7	14	N^{14}	Stable	+n	100
(15)	2	7	7	14	N^{14}	Stable	7	7	14	N^{14}	Stable		14.66
	8	7	7	14	N^{14}	Stable	7	7	14	N^{14}	Stable		
	10	6	6	12	C^{12}	Stable	8	8	16	O^{16}	Stable		
(16)	12	6	6	12	C^{12}	Stable	8	8	16	O^{16}	Stable		35.89
	14	6	6	12	C^{12}	Stable	8	8	16	O^{16}	Stable		
	16	6	6	12	C^{12}	Stable	8	8	16	O^{16}	Stable		
(17)	9	12	12	24	2 C^{12}	Stable	2	2	4	He^{4}	Stable		15.06
(18)	1	2	3	5	He^{4}	0.76(zs)	12	11	23	O^{16}+He^{4}+$2H^{1}$	11.3(s)	+2n	34.38
	8	8	9	17	O^{16}	Stable	6	5	11	$2He^{4}$+$2H^{1}$	20.385(m)	+2n	
	13	12	11	23	O^{16}+He^{4}+$2H^{1}$	11.3(s)	2	3	5	He^{4}	0.76(zs)	+2n	

[1] Decay time of the isotope (half life): zepto-seconds, 10-21 (zs); femto-seconds, 10–15 (fs); seconds (s); minutes (m); hours (h); days (d); years (y)
[2] Picking Option

NVS are summarized in Table 5. The results of the simulation show that the fragments are consistent with those of reaction (2) for fissions occurring along two different planes: 14, 16 (see Table 5 and Fig. 3). It is remarkable that the fragments from the fission along plane 14 are identical to those along plane 16. The simulation produces an isotope

Table 4. Fragments($2\ Al_{13}^{27} + 2$ neutrons)from the simulation of reaction (1).

Fission plane	Fragment 1				Fragment 2					Partial fission probability (%)
	Z_1	N_1	A_1	Isotope	Z_2	N_2	A_2	Isotope		
2	13	14	27	Al^{27}	13	16	29	Al^{27}	+ 2n	10.65
8	13	14	27	Al^{27}	13	16	29	Al^{27}	+ 2n	12.56

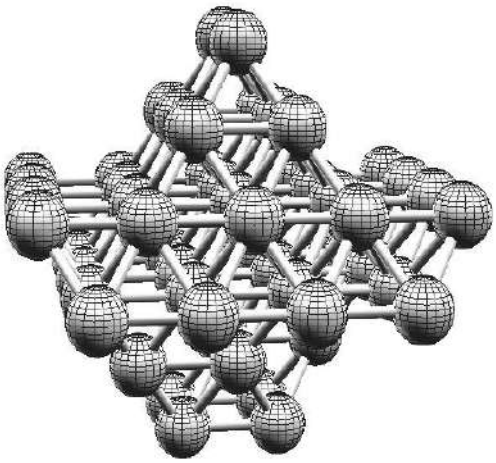

Figure 1. Screenshot of the 3D ^{56}Fe lattice structure built using NVS, which is downloadable from www.res.kutc.kansai-u.ac.jp/ cook.

of Mg and an isotope of Si, which are identified as Fragments 1 and 2. In each case, Fragment 1 is stable, whereas Fragment 2 is unstable. In particular, Fragment 1 is a stable nucleus of Mg^{24} and Fragment 2 is a nucleus of Si^{32}, unstable, which contains four neutrons that can be emitted when reaction (2) occurs.

Considering the data from the Earth's crust and the indirect piezonuclear evidence, reactions (7) and (12) are particularly significant for their implications concerning atmosphere evolution and ocean formation, respectively [9–12]. The simulation results of these reactions are summarized in Table 3. The simulation of piezonuclear reaction (7) produces as fragments two nuclei of C^{12} with no excess of neutrons (Figs. 4 and 5). Therefore, the simulation describes a symmetrical fission that does not entail neutron emissions according to piezonuclear reaction (7).

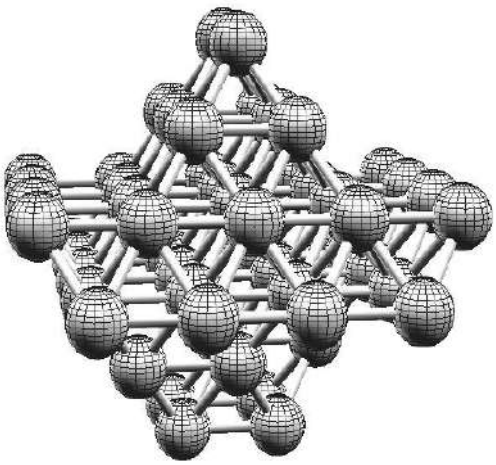

Figure 2. Fracture of the ^{56}Fe lattice along planes 2 ($x = 0$) and 8 ($y = 0$); broken bonds in red between Al fragments of reaction (1) in Table 3.

Table 5. Fragments (Mg_{12}^{24} + Si_{14}^{28}+ 4 neutrons) from the simulation of reaction (2).

Fission plane	Fragment 1				Fragment 2					Partial fission probability (%)
	Z_1	N_1	A_1	Isotope	Z_2	N_2	A_2	Isotope		
14	12	12	24	Mg^{24}	14	18	32	Si^{28}	+4n	20.37
16	12	12	24	Mg^{24}	14	18	32	Si^{28}	+4n	20.37

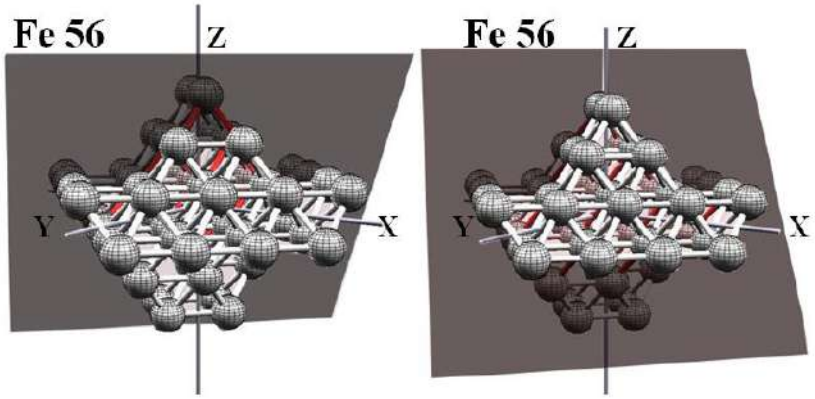

Figure 3. Fracture of ^{56}Fe lattice along planes 14 ($-x-y+z=1$) and 16 ($x+y+z=1$); broken bonds in red between Mg and Si Fragments of reaction (2) in Table 3.

On the other hand, as observed in the case of reactions (1), (2), and (12), there are unstable fragments. In particular, for every plane (Table 3) that allows for the products $2O_8^{16}$ + $4H_1^1$ of piezonuclear reaction (12), at least one of the two fragments obtained from each simulation is unstable. This result suggests that neutron emission is favored in many of the lattice fission events (Figs. 6 and 7).

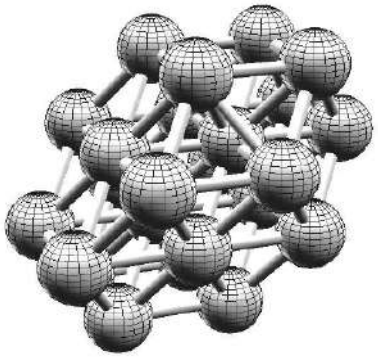

Figure 4. ^{24}Mg nuclear lattice structure.

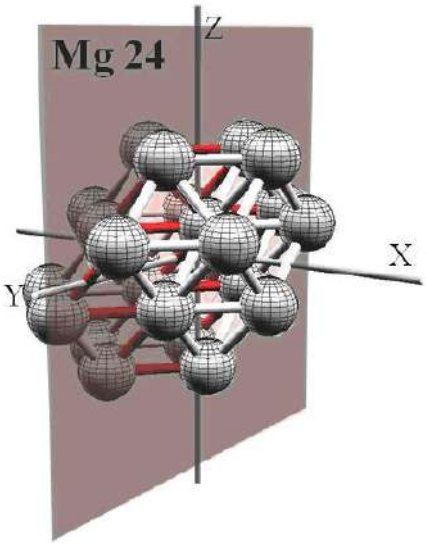

Figure 5. Fracture of the ^{24}Mg lattice along plane 2; broken bonds are represented in red between the fragments of reaction (7) in Table 3.

4. Binding Energy and Probability of Alternative Piezonuclear Fission Reactions

As described above, the nucleus is represented as a lattice where the nodal positions are occupied by the nucleons. A given nuclear lattice in its ground-state has a certain total binding energy (BE) that generally depends on the number and type of nearest-neighbor nucleon–nucleon bonds, thus on the number of constituent nucleons [21,22]. The binding energy is usually expressed as average binding energy per nucleon (BE/nucleon) or average binding energy per bond

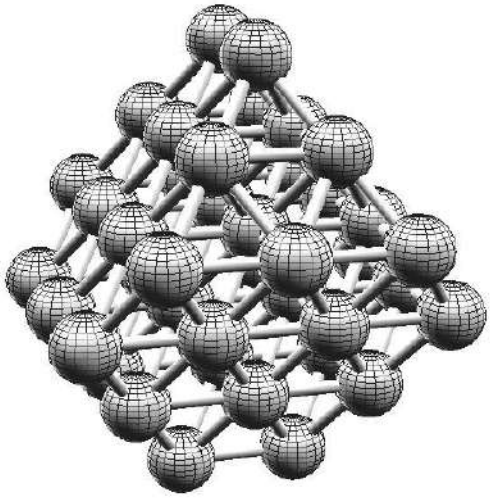

Figure 6. ^{40}Ca nuclear lattice structure.

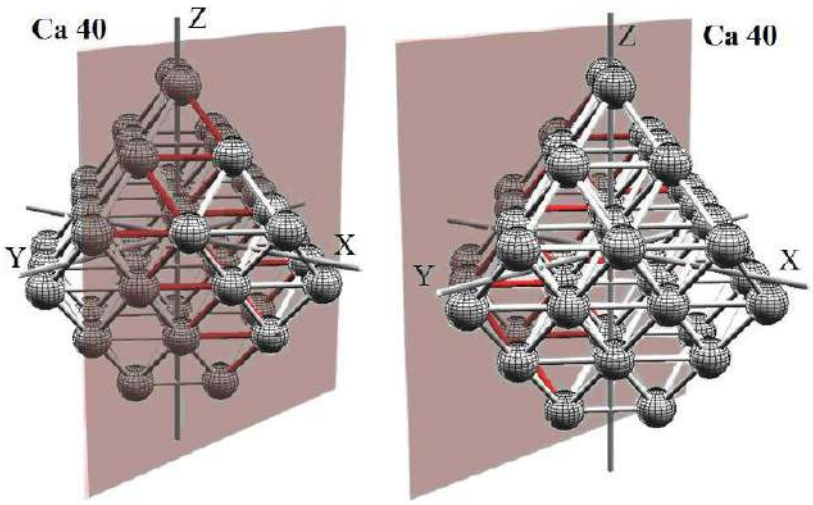

Figure 7. Fracture of ^{40}Ca along planes 1 and 3; broken bonds in red between the fragments of reaction (12) in Table 3.

(BE/bond), which represents a mean value of the energy distribution among the bonds in the nucleus [21,22]. According to the lattice model, the bonds are not all equivalent and are formed by various combinations of nucleon states (as specified by quantum numbers *n, j, m, s* and i). Specifically, the dipole–dipole interactions of nucleon pairs are attractive (singlet-pairs) for all nearest-neighbor PP and NN combinations, but there are both attractive and repulsive dipole combinations for PN pairs (triplet- and singlet-pairs, respectively). As a consequence, the antiferromagnetic fcc lattice with alternating proton-neutron layers implies the existence of lattice planes that are either strongly or weakly bound, depending on the character of the bonds in the lattice plane. It is the internal structure of the nucleon lattice that leads directly to the prediction of lattice fragments of various masses and probabilities.

In order to assess the probability of fission occurring in a given nucleus, it is necessary to know the binding force of the nuclear lattice structure: the lower is this force the higher is the probability of fission. This can be evaluated in terms of binding energy of the lattice structure through a specific plane. In particular, the binding energy of the bonds between nearest-neighbor nucleons crossed by a fracture plane minus the Coulomb repulsion through the same plane represents the residual binding energy. Inverting this value yields a ratio (MeV^{-1}) that is defined as proportional to the probability of fission ($P_{fission}$) [17]:

$$P_{\text{fission}}\,(Z,N) = \frac{1}{\left(\beta \sum_{m}^{A_{\text{f1}}} \sum_{n}^{A_{\text{f2}}} b_{m,n} - \sum_{j}^{Z_{\text{f1}}} \sum_{k}^{Z_{\text{f2}}} Q_{j,k}\right)}, \tag{4}$$

where Z, N, and A are the number of protons, neutrons and the total number of nucleons contained in the atomic nucleus; f1 and f2 stand for the two resulting fragments of the given reaction; β is an experimental value of the nucleon–nucleon binding force. Between nearest-neighbor nucleons this value changes according to the different nature of the bond; $b_{m,n}$ is the number of bonds across the fission plane taken into consideration and so the number of broken nucleon–nucleon bonds along the fracture plane; $Q_{j,k}$ is the Coulomb repulsive contribution between the protons in the two fragments defined by the fission plane.

Using the parameter P_{fission}, the probabilities of piezonuclear reactions (1) and (2) were calculated as shown in

detail in Tables 4 and 5 and summarized in Table 3. The Fission Probability is expressed as a normalized percentage of the cases studied for each element reported in Table 2 with their relevant fission planes, and a given binding force value β is assumed (approximately comprised in the range between 2 and 4 MeV) [17]. From Table 4, the simulation of piezonuclear reaction (1) results in two cases of the 17 possible fission planes, with a total P_{fission} of $\sim$23%, whereas from Table 5 it is observed that reaction (2) results in two cases having a total P_{fission} of $\sim$41%. According to these considerations, it is of interest that these probabilities reproduce the known abundances of the Al^{27}, Mg^{24} and Si^{28} elements in the Earth's crust [9–12]. The probability that a nucleus of Fe^{56} produces Magnesium and Silicon (piezonuclear reaction (2) in Table 2) is significantly larger (ratio: 1.74) than that implying the symmetrical nuclear fission of Fe^{56} into two Al^{27} atoms (reaction (1) in Table 2). This is in agreement with the evidence regarding the compositional changes in the evolution of the Earth's crust. In fact, the total decrease in Fe^{56} over the last 4.57 Billion years of about 11% seems to be consistently counterbalanced by the increases in Mg, Si and Al, where the contribution of Mg^{24} and Si^{28} $\sim$7% is a little less than twice that of the Al^{27} increase, $\sim$4% [9–12]. The ratio of the normalized P_{fission} of reaction (2) to that of reaction (1) is approximately 1.75, as the ratio of Mg and Si ($\sim$7%) increase to the increase in Al ($\sim$4%) in the Earth's crust. It is also interesting to note that reaction (3) involving Fe as the starting element and Ca and C as the resultants can be obtained by the NVS simulation. This reaction, not so frequent in the Earth's crust system, could be recognized as a fundamental reaction during the application of ultrasound to sintered Ferrite (α-Iron) and steel bars, as recently reported by Cardone et al. [33]. This evidence indicates that the NVS is able to reproduce different piezonuclear fission reactions also belonging to different systems and experiments at different scales (Earth's crust or ferrite bar).

The results obtained from the Ca-based reaction simulations also showed consistency with the findings reported in [9–12]. During the evolution of the Earth's crust, Ca decreased by about $\sim$4%, while K increased by about $\sim$2.7%, according to reaction (11). The total Ca depletion may be almost perfectly counterbalanced considering the increases in O and H (H_2O) that together correspond to an increment of about 1.3% [9–12]. This means that more than two thirds of the Ca depletion resulted in potassium and approximately one third in H_2O. On the other hand, considering the probability of fission computed for reactions (10)– (12) by NVS (Table 3), the piezonuclear reaction involving K as the product, reaction (11), returned a normalized probability of $\sim$58.4%. The normalized probability of the simulation of reaction (12), involving H and O as products, is about 31.2% (see Table 3) [9–12]. The ratio of the fission probability of reaction (11) to that of reaction (12) is about two, which is in good agreement with the evidence concerning the Earth's crust [9-12].

The consistency with the evidence drawn from the Earth's crust can be verified also in the case of Mg as the starting element of the anomalous reactions (7)–(9). In particular, we find a global Mg decrease ($\sim$7.9%) that is counterbalanced by a $\sim$2.7% increase in Na in the Earth's crust and by increases of $\sim$2.0% and $\sim$3.2% in H_2O and C, respectively, in the ancient atmosphere. The evidence of the Na increase is supported by the NVS simulation that returns a normalized probability percentage for reaction (8) equal to $\sim$31.0%. With regard to the other reactions, involving C, O and H as resultants, we obtained a total normalized probability percentage of about $\sim$69%. These last two percentages are in good agreement with the considerations concerning the evolution of the Earth's crust composition as about two thirds of the Mg decrease can be ascribed to the formation of gaseous elements such as C and H_2O that formed in the proto-atmosphere of our planet [9–11,34].

5. Conclusions

The simulations conducted using the NVS reproduced the piezonuclear reactions assumed and observed in both laboratory tests and Earth's crust by Carpinteri et al. [1–12]. The results were obtained using the approach recently proposed by Cook and co-workers to provide a fully quantum mechanical unification of the different models of nuclear structure [17,20].

It is true that the full comprehension of the mechanisms is yet to be achieved. However, a possible, yet not intuitive, way to explain the nuclear evidence is to consider the fracture as the origin of the phenomena of neutron emission and isotopic changes, but not the direct cause. Acoustic emissions sources, at very high frequencies (THz), generated by micro and macro-cracks during damage, could be considered as the generating mechanism. The achievement of the acoustic resonance of the atom could lead to the nuclear anomalies in fracture experiments phenomena encountered.

The simulations suggest that neutron emissions can be favored when the product fragments present unstable conditions. From this point of view, the recent evidence provided by fracture and fatigue experiments indicates neutron emissions far in excess of the background level [1–12]. This may be correlated to piezonuclear fission of nuclei along specific weak planes of the lattice structure. Furthermore, the presence of relatively weakly-bound planes within the lattice can be assumed as an indicator of the lattice behavior, through a given plane, calculated by means of the Fission Probability. This implies that certain piezonuclear reactions may occur with a higher probability than others. In particular, the total decrease in Fe^{56} over the last 4.57 billion years of about 11% consistently counterbalanced by an increase in Mg^{24} and Si^{28} ($\sim$7%), and by that in Al^{27} ($\sim$4%), is confirmed by the normalized fission probabilities of the relevant reactions computed by the lattice model. Analogously, similar numerical results obtained by NVS supported the decreases in Ca and Mg and the increases in K, Na, C and H_2O, contributing to explain the Earth's crust evolution together with the proto-atmosphere compositions and the formation of the oceans under the light of the piezonuclear conjecture.

Finally, the current version of the NVS simulates the fission of nuclei assuming an average value of the nuclear binding force. More precise results could be obtained in the case of these reactions using an improved version of the NVS that is able to consider the binding energy between nucleons as a function of the different nucleon states. Such improvements will be implemented in future research in order to take into consideration a more realistic distribution of the binding energy across the nucleus.

References

[1] A. Carpinteri, F. Cardone and G. Lacidogna, Piezonuclear neutrons from brittle fracture: Early results of mechanical compression tests, *Strain* **45** (2009) 332–339; Atti dell'Accademia delle Scienze di Torino, Torino, Italy **33** (2009) 27–42.

[2] F. Cardone, A. Carpinteri and G. Lacidogna, Piezonuclear neutrons from fracturing of inert solids, *Phys. Lett*. A **373** (2009) 4158–4163.

[3] A. Carpinteri, F. Cardone, G. Lacidogna, Energy emissions from failure phenomena: Mechanical, electromagnetic, nuclear, *Experimental Mechanics* **50** (2010) 1235–1243.

[4] A. Carpinteri, O. Borla, G. Lacidogna and A. Manuello, Neutron emissions in brittle rocks during compression tests: Monotonic vs. cyclic loading, *Physical Mesomechanics* **13** (2010) 268–274.

[5] A. Carpinteri, G. Lacidogna, A. Manuello and O. Borla, Energy emissions from brittle fracture: Neutron measurements and geological evidences of piezonuclear reactions, Strength, *Fracture and Complexity* **7** (2011) 13–31.

[6] A. Carpinteri, G. Lacidogna, A. Manuello and O. Borla, Piezonuclear fission reactions: Evidences from microchemical analysis, neutron emission, and geological transformation, *Rock Mechanics and Rock Engineering* **45** (2012) 445–459.

[7] A. Carpinteri, G. Lacidogna, , O. Borla, , A. Manuello and G. Niccolini, Electromagnetic and neutron emissions from brittle rocks failure: Experimental evidence and geological implications, *Sadhana* **37** (2012) 59–78.

[8] A. Carpinteri, G. Lacidogna, A. Manuello and O. Borla, Piezonuclear fission reactions from earthquakes and brittle rocks failure: Evidence of neutron emission and nonradioactive product elements, *Experimental Mechanics*, doi: 10.1007/s11340-012-9629-x (2012c).

[9] A. Carpinteri, A. Chiodoni, A. Manuello and R. Sandrone, Compositional and microchemical evidence of piezonuclear fission reactions in rock specimens subjected to compression tests, *Strain* **47**(2) (2011) 267–281.

[10] A. Carpinteri and A. Manuello, Geomechanical and Geochemical evidence of piezonuclear fission reactions in the Earth's Crust, *Strain* **47** (2011) 282–292.

[11] A. Carpinteri and A. Manuello, An indirect evidence of piezonuclear fission reactions: Geomechanical and geochemical

evolution in the Earth's crust, *Physical Mesomechanics* **15** (2012) 14–23.
[12] N.D. Cook,A. Manuello, R. Sandrone, S. Guastella, O. Borla, G. Lacidogna and A. Carpinteri, Neutron emissions and compositional change evidence in piezonuclear reactions during fracture of granite, basalt and magnetite fracture tests (This issue).
[13] A. Widom, J. Swain and Y.N. Srivastava, Photo-disintegratin of the iron nucleus in fractured magnetite rocks with magetostriction, arXiv: 1306.6286v1 (2013).
[14] A. Widom, J. Swain and Y.N. Srivastava, Neutron production from the fracture of piezoelectric rocks, *J. Phys. G: Nucl. Part. Phys.* **40** (2013) doi:10.1088/0954-3899/40/1/015006.
[15] P.W. Bridgman, The breakdown of atoms at high pressures, *Phy. Rev*. **29** (1927) 188–191.
[16] E. Storms, *Science of Low Energy Nuclear Reaction: A Comprehensive Compilation of Evidence and Explanations About Cold Fusion* (World Scientific, Singapore, 2007).
[17] N.D. Cook, *Models of the Atomic Nucleus* (Springer, Hideldburg, 2^{nd} Ed., 2010).
[18] N.D. Cook and V. Dallacasa, Face-centered-cubic solid-phase theory of the nucleus, Phy. Rev. C **35** (1987) 1883.
[19] N.D. Cook and V. Dallacasa, LENR and nuclear structure theory, *Proc. ICCF-17*, August 12–17, 2012, Daejong, Korea.
[20] T. Mizuno, Nuclear Transmutation: The reality of cold fusion, Tuttle, Concord NH (1998).
[21] J. Lilley, *Nuclear Physics: Principles and Applications* (Wiley, New York, 2001).
[22] K.S. Krane, *Introductory Nuclear Physics* (Wiley, New York, 1987).
[23] N.D. Cook, An FCC lattice model for nuclei, *Atomkernenergie* **28** (1976) 195.
[24] N.D. Cook, Quantization of the FCC nuclear theory, *Atomkernenergie* **40** (1981) 51.
[25] V. Dallacasa and N.D. Cook, The FCC nuclear model (II), *Nuovo Cimento II* 97 (1987) 157.
[26] N.D. Cook, Computing nuclear properties in the FCC model, *Computers in Phys.* **3** (1989) 73.
[27] N.D. Cook, Nuclear binding energies in lattice models, *J. Phys. G* **20** (1994) 1907.
[28] N.D. Cook, Is the lattice gas model a unified model of nuclear structure? *J. Phys.* **25** (1999) 1.
[29] N.D. Cook, Toward an explanation of transmutation products on palladium cathodes, *Proc. ICCF-14*, 2008, Rome, Italy.
[30] N.D. Cook, Simulation of palladium fission products using the FCC lattice model, *Proc. ICCF-16*, 2010, Chennai, India.
[31] E. Wigner, On the consequences of the symmetry of the nuclear hamiltonian on the spectroscopy of nuclei, *Phy. Rev.* **51** (1937) 106.
[32] T. Mizuno, Experimental confirmation of the nuclear reaction at low energy caused by electrolysis in the electrolyte, *Proc. Symp. on Advanced Research in Energy Technology,* 2000, pp. 95–106.
[33] F. Cardone, A. Carpinteri, A. Manuello, A. Mignani, R.A. Sepielli and M. Petrucci, Ultrasonic Piezonuclear Reactions in Iron, This issue.
[34] L. Liu, The inception of the oceans and CO_2-athmosphere in the early history of the Earth. Earth Planet, *Sci. Lett.* **227** (2004) 179–184.